The Reaction between Mn and Se Layers

Marisa A. Choffel, [a] Danielle M. Hamann, [a] Jordan A. Joke, [a] Dmitri Leo M. Cordova, [a] and David C. Johnson*[a]

Dedicated to Professor Wolfgang Bensch on the occasion of his 65th Birthday

Abstract. The mechanism of the reaction between Mn and Se is shown to depend on the composition and the thickness of Mn and Se layers. Samples were prepared by modulated elemental reactants (MER) method. The elements were evaporated using either electron beam guns or effusion cells and the total amount of each element was controlled using quartz crystal monitors. Different ratios of the elements and different total amounts of the elements per repeating unit were experimentally explored. Near a one to one ratio of Mn and Se, α -MnSe crystallizes upon deposition. Compositions near a one to two

ratio of Mn to Se proceed through an amorphous intermediate for the layer thicknesses investigated, with MnSe₂ crystallizing at 150 °C. Between these compositions, the two bilayer thicknesses explored evolve differently, with films with bilayer thicknesses near 0.5 nm nucleating MnSe, whereas films with bilayer thicknesses around 1 nm nucleating a mixture of MnSe and MnSe₂. Samples around 80% Se formed a previously unreported compound with a small monoclinic unit cell with lattice parameters a = 4.942(2) Å, b = 4.32(3) Å, c = 3.779(1) Å, and $\beta = 90.13(3)^{\circ}$.

Introduction

In general, the formation of crystalline solids from the elements or via the reaction between compounds is not well understood.^[1-3] While there is a consensus that interdiffusion, nucleation, and growth are key parts of the formation process, there is little understanding of how these fundamental reaction steps can be controlled with experimental parameters. This knowledge is crucial for planning a directed synthesis.^[4] A promising approach to investigate the formation mechanism of crystalline solids is based on using precursors containing alternating layers of the elements.^[5] An advantage of this approach, called modulated elemental reactants^[6] or nano-alloying^[7] is the ability to form a homogeneous, amorphous intermediate. [8] Synthetically accessible metastable compounds need to be more stable than an amorphous intermediate of the same composition. [9] Fortunately, the composition of amorphous intermediates can be systematically controlled to influence which compounds nucleate first.[10-12] This has enabled the synthesis of a number of metastable compounds.^[13]

The Mn-Se system has been the subject of multiple recent investigations using epitaxial growth techniques [14–16] and solution phase synthesis approaches, [14,15,17–21] which were driven by the desire to make discrete magnetic layers, magnetic nanoparticles, or diluted magnetic semiconductors. [22–24] Only two thermodynamically stable compounds are known in the Mn-Se system. Both can be prepared using traditional high temperature reactions of the elements. [25,26] The monoselenide, α -MnSe, has a sodium chloride crystal structure and the diselenide, MnSe₂, has a cubic pyrite structure. In both com-

pounds Mn is octahedrally coordinated by Se. In α -MnSe, Se is octahedrally coordinated by Mn. In MnSe₂, there are discrete Se₂ dimers, and the Se is tetrahedrally coordinated by one Se atom and three Mn atoms. These structures are closely related. Replacing the Se dimers in the pyrite by Se atoms at the center of mass of the Se dimmers, results in the rock salt structure. In addition to the two thermodynamically stable compounds, two metastable MnSe polymorphs (β -MnSe and γ -MnSe) have been reported to form as nanocrystals from solutions. [27,28]

The purpose of the presented investigation is to study the formation mechanisms of MnSe and MnSe2 from multilayered Mn-Se precursors, where the ratio of the elements and the total amount of elements per repeating layer were varied to determine parameters required to form amorphous reaction intermediates and to discover if any metastable compounds nucleate at low reaction temperatures. A number of films with different ratios of Mn and Se were prepared with two bilayer thicknesses. Alternating layers of Mn and Se were deposited to obtain the four target compositions and different bilayer thicknesses. The bilayers were repeated multiple times to increase the sample volume. The evolution of the films as a function of temperature was followed using X-ray diffraction. The sequence of phase formation changed with both composition and bilayer thickness. MnSe formed from films that were close to a one to one ratio of Se and Mn during the deposition. For compositions containing ca. 60% Se, an amorphous intermediate formed and the first compound crystallized depended on bilayer thickness. MnSe formed first in the film with thin bilayers, whereas a mixture of MnSe₂ and MnSe formed in the film with thicker bilayers. Both the thin and thicker bilayer films with a 1:2 ratio of Mn to Se were amorphous as deposited and the first crystalline compound formed was MnSe₂ from both precursors. Both of the films with initial composi-

^{*} Prof. D. C. Johnson E-Mail: Davej@uoregon.edu

[[]a] Materials Science Institute and Department of Chemistry University of Oregon Eugene, OR, USA

tions of ca. 80% Se formed a new metastable compound whose diffraction pattern was consistent with a monoclinic unit cell. These results show that amorphous intermediates can be formed from precursors with thin bilayer thicknesses and that both the composition and the bilayer thickness influence which compound nucleates first.

Results and Discussion

A number of precursor films were prepared with systematic changes in composition and layer thickness to probe how the reaction mechanism varies as a function of these experimental parameters. One set of precursors was prepared, where the bilayer MnlSe thicknesses were on the order of that require to form a single unit cell of MnSe or MnSe₂. Four films (A1 – D1) were made with compositions shown in Figure 1. A second set of four precursors (A2 – D2) was prepared with bilayer thicknesses approximately twice that of the precursors A1 – D1 with similar compositions (see Figure 1). X-ray reflectivity scans of the as deposited samples contained only a few Kiessig fringes. While there were enough Kiessig fringes to determine the film thickness, the termination of fringes at 2.5 to 6.5 degrees indicates a surface roughness of ca. 20 Å calculated using the approach of Parratt.^[29]

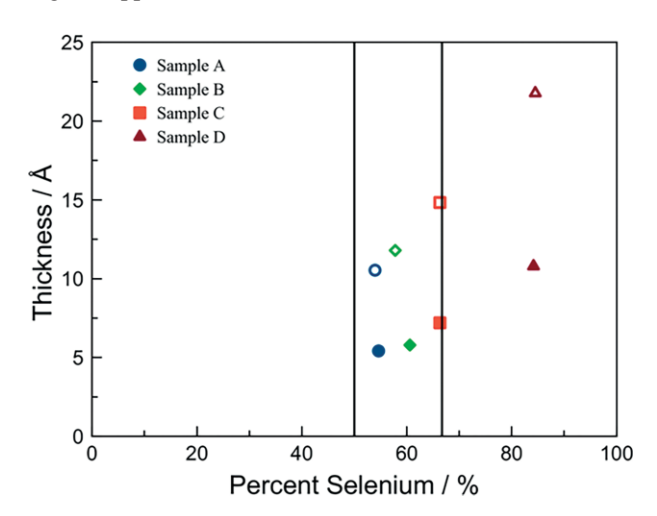
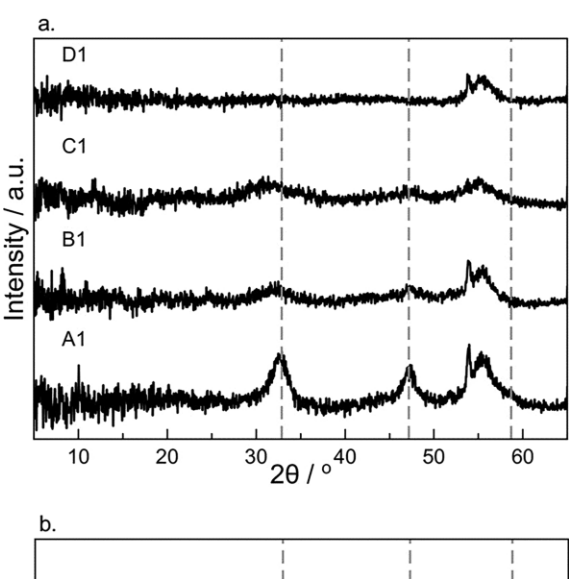


Figure 1. Summary of the composition and thickness of the prepared precursors.

The grazing incidence diffraction patterns of the as deposited precursors are shown in Figure 2. The diffraction patterns of the two samples with a starting composition of 54% selenium, A1 and A2, indicated that both crystallized α -MnSe during the deposition. Distinct reflections at 32.9 and 47.2° from the (200) and (220) reflections and a weak reflection at 58.7° from the (222) reflection are apparent in the scans. The vertical dashed lines in Figure 2 indicate the locations of these reflections for α -MnSe. In addition to the α -MnSe reflections, there is a broad maximum centered at ca. 55° with a sharp maximum at 54° that are assigned to a surface component, as these features are not apparent in specular diffraction scans. We suspect that this feature is due to a surface oxide from the magnitude of the intensity of the oxygen signal in the XRF

data. This surface component is present in all of the as deposited samples. The rest of the samples, all more Se rich than A1 and A2, have much broader and weaker maxima in the as deposited scans, suggesting that they may be amorphous as deposited. The broad maximum at ca. 32° shifts to a lower angle as the samples become more Se rich. Even for the B samples this maximum is at an angle lower than that expected for the (200) reflection of α -MnSe.



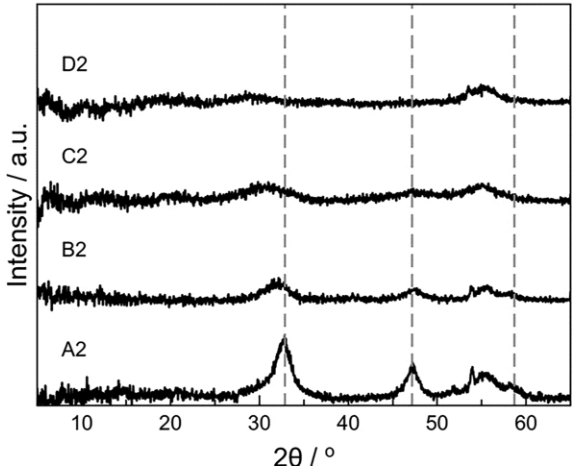


Figure 2. Grazing incidence diffraction scans of the eight precursors before any annealing; (a) films A1 - D1 and (b) films A2 - D2. The dashed vertical lines at 32.9, 47.2, and 58.7° mark the locations of the (200), (220), and (222) reflections of the α -MnSe.

All of the samples were annealed at sequentially higher temperatures to follow the evolution of the films. Diffraction patterns and X-ray fluorescence (XRF) data were obtained after each annealing temperature. The XRF data for samples A1 and A2 showed that the initial films were 54% Se and 46% Mn. The Se content of the films decreased due to sublimation of Se between 100 and 250 °C. The composition of the films remained approximately constant between 250 and 400 °C, slightly Mn rich relative to the stoichiometry of MnSe. This difference is presumably due to the presence of a Mn oxide on the surface of the samples. Both samples showed increasing oxygen content and decreased Se content after annealing at

450 °C. Figure 3 contains the diffraction patterns collected during the annealing study for samples A1 and A2.

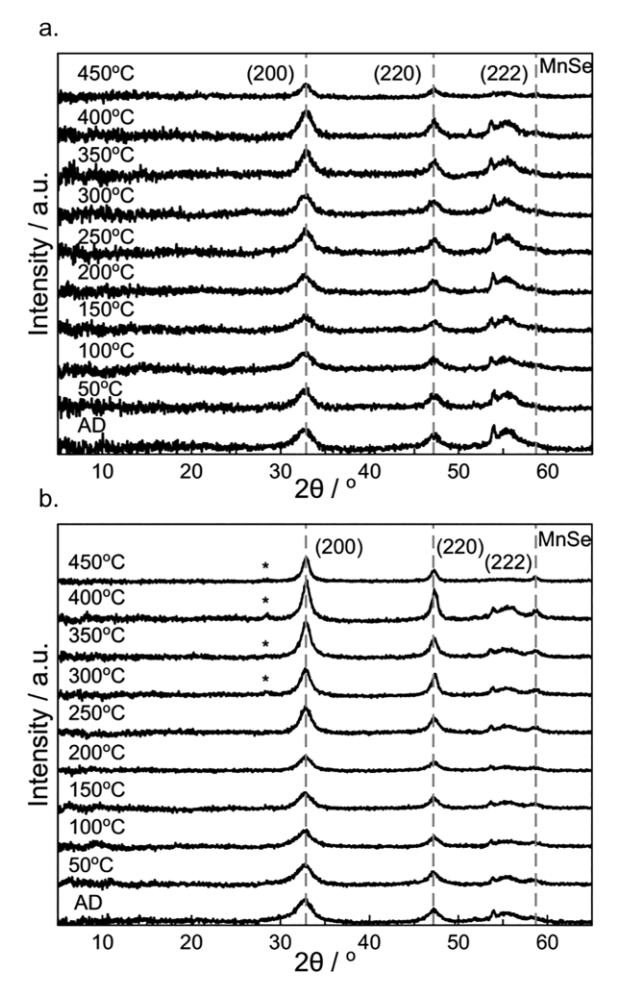


Figure 3. Grazing incidence diffraction scans collected for samples A1 (a) and A2 (b) as a function of annealing temperature. The (111) reflection of α -MnSe is marked by an asterisk.

For both the A1 and A2 sample, the reflections of MnSe in the as deposited films sharpen and increase in intensity as the annealing temperature is increased. In sample A2, the weak (111) reflection of MnSe becomes visible after annealing at 300 °C, reflecting the increasing crystallinity of the samples. There is a decrease in the intensity of the Bragg reflections at 450 °C, which is correlated with an increase in the oxygen fluorescence signal and decrease in Se fluorescence as measured by XRF. This annealing data confirms that the as deposited films of both thicknesses formed MnSe on deposit, even though the films contained extra Se. The lattice parameter of the MnSe in both samples [5.44(1) Å] is independent of annealing temperature and in agreement with the 5.45 Å cubic unit cell reported in the literature.^[30] This data suggests that it will be difficult to obtain amorphous films with compositions near a 1 to 1 ratio of Mn to Se using modulated precursors.

Samples B1 and B2, which were approximately 60% Se and 40% Mn as deposited, evolved differently due to their different bilayer thicknesses. Figure 4 contains the grazing incidence diffraction scans collected from these samples after each an-

nealing temperature. In sample B1, which is slightly more Se rich than sample B2, the broad diffraction maxima present in the as deposited film change, becoming consistent with the formation of MnSe after annealing at 150 °C. Sample B2, which has thicker bilayers and is slightly more Mn rich than sample B1, forms a mixture of MnSe₂ and MnSe during this annealing step. This may be a consequence of a non-uniform composition in sample B2 due to the thicker bilayers.

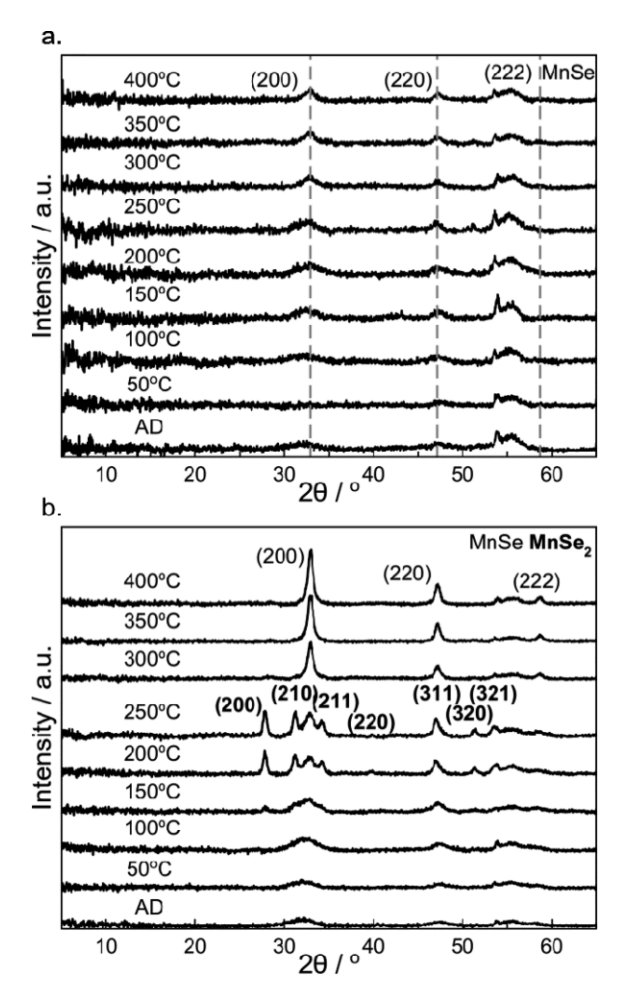


Figure 4. Grazing incidence diffraction scans of samples B1(a) and B2 (b) as a function of annealing temperature.

The MnSe₂ lattice parameters determined from the diffraction scans for sample B2 are smaller [6.40(1) Å] than the literature value of c = 6.417 Å. [^{26]} During the higher temperature anneals, sample B1 behaves similarly to sample A1. The rate of Se loss decreases during the 250 and 400 °C anneals, with its composition becoming Mn rich relative to MnSe, presumably due to a surface oxide. The MnSe reflections become sharper and more intense as annealing temperature is increased. During the 200 and 250 °C annealing of sample B2, the reflections of MnSe₂ sharpen and grow in intensity. There is Se loss during the 300 °C annealing of sample B2, and the diffraction pattern after this anneal shows a significant increase in the intensity of MnSe reflections. Only reflections for MnSe are visible in the diffraction patterns obtained after the 350 °C anneal. The sample after annealing at 400 °C has a composi-

tion of 52 % Mn and 48 % Se, with the excess Mn again due to the existence of a surface oxide.

Precursors C1 and C2 behaved similarly as a function of annealing temperature. They were both amorphous and had compositions close to stoichiometry of MnSe₂ as deposited. As shown in Figure 5, both samples formed MnSe₂ after annealing at 150 °C. The MnSe₂ lattice parameter 6.41(1) Å, determined from the diffraction patterns of both samples, matches the literature value of 6.417 Å. [26] To decrease the loss of Se from sublimation, sample C2 was covered with a silicon wafer, while C1 was not. As a consequence, sample C1 loses Se at a much faster rate as a function of annealing temperature than sample C2 and reflections for MnSe are visible at a much lower annealing temperature. The ratio of Mn to Se in sample C2 remained near a 1 to 2 ratio until 350 °C. After annealing at 400 °C, the ratio of Mn to Se changed, becoming 1 to 1.1. After this annealing temperature MnSe was the dominant compound in the diffraction pattern.

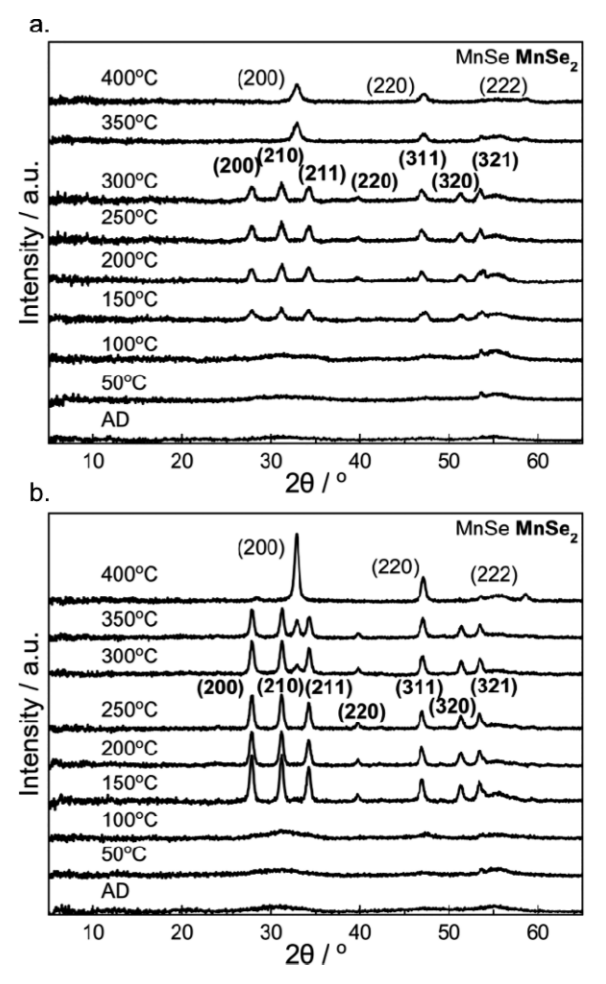


Figure 5. Grazing incidence diffraction scans collected from samples C1 (a) and C2 (b) as a function of annealing temperature.

Precursors D1 and D2 surprised us, forming a compound not found on the equilibrium phase diagram during the annealing study. The as deposited precursors were both greater than 80% selenium and the equilibrium phase diagram indicates they should evolve to form a mixture of MnSe₂ and Se. Both

samples were amorphous as deposited and did not change during the 50 and 100 °C annealing as shown in Figure 6. Both samples form a previously unreported compound on annealing at 150 °C, and all the reflections in both samples can be indexed to a small monoclinic unit cell with lattice parameters a = 4.942(2) Å, b = 4.32(3) Å, c = 3.779(1) Å, and $\beta = 90.13(3)$ °. The relative intensities of the reflections, however, are different in the two scans, suggesting that there may be different amounts of preferred orientation or there may be different relative occupancies of crystallographic sites in the two samples.

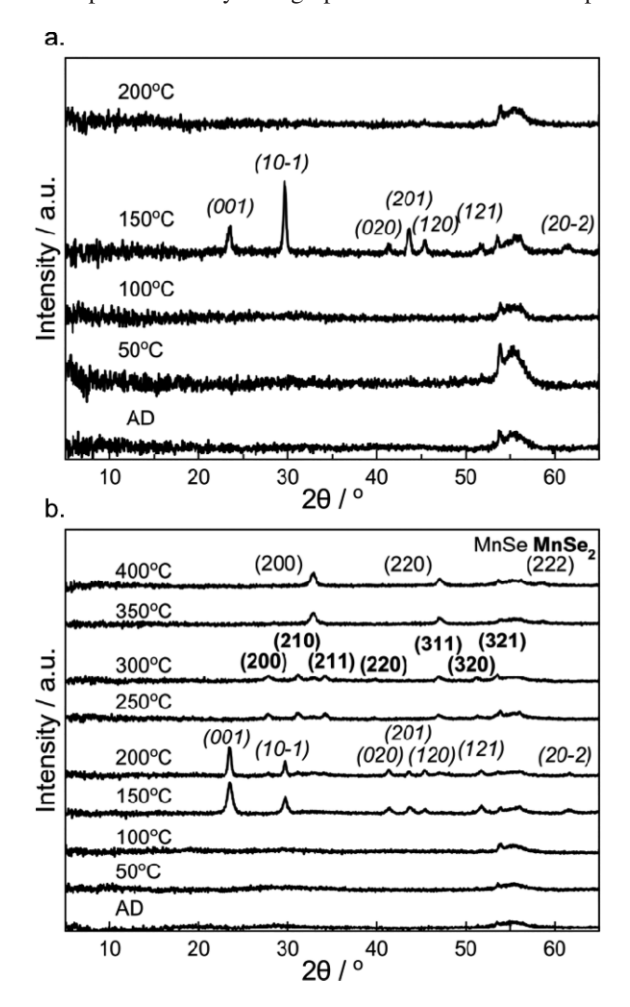


Figure 6. Grazing incidence diffraction scans of samples D1 (a) and D2 (b) as a function of annealing temperature.

The composition of the D1 sample is close to a 1 to 2 ratio of Mn to Se as a result of significant Se loss during annealing at 150 °C. This suggests that the composition of the new compound is likely to be near a 1 to 2 ratio of Mn to Se. The composition of the D2 sample did not change significantly on annealing at 150 °C, perhaps as a consequence of it being much thicker than sample D1. After annealing at 200 °C, the diffraction pattern of sample D2 has small reflections consistent with the formation of MnSe₂ and the reflections for the new compound have sharpened. After annealing at 200 °C, the diffraction pattern of sample D1 is very different, without any sharp reflections. The XRF data indicates that sample D1 lost a significant amount of Se at this annealing temperature, with

a final composition close to 1 to 1 between Mn and Se. At 250 °C, the diffraction pattern for sample D2 contains reflections consistent with a film of MnSe₂ and the composition from the XRF data is consistent with this. At higher annealing temperatures, sample D2 behaves similar to sample C2, losing Se and forming MnSe.

There are several differences between the samples with thinner bilayers (A1 – D1) and those with thicker bilayers (A2 – D2). The samples with thinner bilayers all lose Se at a faster rate than the samples with thicker bilayers. Since samples A1 – D1 are all much thinner in total thickness than A2 – D2, this suggests that Se loss is limited by diffusion of Se to the surface. The samples with thinner bilayers also end up being more Mn rich (and Se poor) relative to the samples with thicker bilayers. We believe that this is due to the Mn containing oxide forming on surface of the samples. Since the samples with thinner bilayers are also thinner in total thickness, this oxide consumes a larger fraction of the total Mn in the film.

Previous investigations using modulated elemental reactants indicated that there is a critical bilayer thickness, with precursors layered below the critical thickness forming amorphous intermediates and those layered above the critical thickness nucleating binary compounds at the interface between elemental layers.^[31] The results of the annealing studies as a function of composition and bilayer thickness of the Mn-Se samples suggest that the critical bilayer thickness in this system is a function of composition. Both the thicker and the thinner samples closest in composition to the stoichiometry of MnSe (A1 and A2) formed MnSe during the deposition. The samples with ca. 60% Se, B1 and B2, were X-ray amorphous but evolved differently. We suspect that at this composition sample B1 was below the critical thickness, while sample B2 was above the critical thickness. All of the samples with a lower Mn to Se ratio formed amorphous intermediates. The thicker and thinner bilayer samples (C1 and C2, D1 and D2) nucleated the same first compound.

Conclusions

This study showed that it is possible to form amorphous Mn-Se intermediates from modulated elemental reactants if they are more than 60% Se. The critical bilayer thickness at this composition is on the order of 1 nm. Films that were more Mn rich formed MnSe during deposition. Films that were more Se rich formed amorphous intermediates and no difference in the evolution of the films were observed for bilayer thicknesses less than 2 nm. In the most Se rich films investigated, a new metastable compound was discovered. The diffraction pattern can be indexed to a monoclinic unit cell with lattice parameters of a = 4.942(2) Å, b = 4.32(3) Å, c = 3.779(1) Å, and $\beta = 90.13(3)^{\circ}$.

Experimental Section

The precursors were synthesized using a vacuum depositions chamber operating at pressures below 5×10^{-7} Torr. Manganese was deposited using an electron beam gun and selenium was deposited using a Knud-

son effusion cell. All films were deposited on silicon wafers with a native oxide layer. Deposition was controlled using quartz crystal microbalances (QCM) to monitor the rate of deposition and the amount of material deposited in each layer. Different amounts of manganese and selenium were deposited for each precursor in order to target four different compositions. For each of the compositions investigated, precursors with two different bilayer thicknesses were prepared. Twenty-four bilayers were deposited in each precursor.

The samples were annealed at each temperature for 30 min on a hot plate in a nitrogen atmosphere with an oxygen pressure of less than 1 ppm. The initial annealing temperature was 50 °C and the annealing temperatures were increased in steps of 50 °C. X-ray reflectivity, X-ray fluorescence and grazing incidence X-ray diffraction scans were collected after each annealing step. X-ray reflectivity was collected using a Bruker D8 Discover diffractometer using $\text{Cu-}K_a$ radiation. Grazing incidence X-ray diffraction (XRD) scans were collected with a Rigaku SmartLab with a Cu source. X-ray fluorescence data was collected with a Rigaku ZSX Primus-II with a rhodium X-ray tube.

Calibration samples containing Mn and Se were annealed in a selenium atmosphere, forcing the formation of pure MnSe₂ films as confirmed by diffraction scans. The X-ray fluorescence intensity of both Mn and Se were measured. Since the proportionality factor between Se intensity and the number of Se atoms per unit area was known from an earlier study,^[32] we could calculate the number of Se atoms per unit area in each sample. The number of manganese atoms/ unit area in each sample was calculated from this using the stoichiometric ratio between manganese and selenium. The linear relationship between XRF intensity and atoms per unit area for both Mn and Se were used to determine the composition of the films in this study.

Acknowledgements

This material is based upon work supported by the National Science Foundation Graduate Research Fellowship Program under Grant No. 1309047. The authors acknowledge support from the National Science Foundation under grant DMR-1710214. We would like to acknowledge the Center for Advanced Materials Characterization in Oregon (CAMCOR) at the University of Oregon.

Keywords: Metastable; Manganese; Selenium; Amorphous; Intermediates

References

- S. Kraschinski, S. Herzog, W. Bensch, Solid State Sci. 2002, 4, 1237–1243.
- [2] S. Herzog, S. Kraschinski, W. Bensch, Z. Anorg. Allg. Chem. 2003, 629, 1825–1832.
- [3] M. Behrens R. Kiebach, W. Bensch, D. H. Jäger, 45 (6), 2704– 2712.
- [4] M. Regus, G. Kuhn, S. Polesya, S. Mankovsky, M. Alemayehu, M. Stolt, D. C. Johnson, H. Ebert, W. Bensch, Z. Kristallogr., Cryst. Mater. 2014, 229, 505–515.
- [5] M. Fukuto, M. D. Hornbostel, D. C. Johnson, J. Am. Chem. Soc. 1994, 116, 9136–9140.
- [6] M. Regus, S. Mankovsky, S. Polesya, G. Kuhn, J. Ditto, U. Schürmann, A. Jacquot, K. Bartholomé, C. Näther, M. Winkler, J. D. König, H. Böttner, L. Kienle, D. C. Johnson, H. Ebert, W. Bensch, J. Solid State Chem. 2015, 230, 254–265.
- [7] J. D. König, M. Winkler, S. Buller, W. Bensch, U. Schürmann, L. Kienle, H. Böttner, J. Electron. Mater. 2011, 40, 1266–1270.

- [8] T. Novet, D. C. Johnson, J. Am. Chem. Soc. 1991, 113, 3398-3403
- [9] W. Sun, S. T. Dacek, S. P. Ong, G. Hautier, A. Jain, W. D. Richards, A. C. Gamst, K. A. Persson, G. Ceder, *Sci. Adv.* **2016**, 2, e1600225–e1600225.
- [10] O. Oyelaran, T. Novet, C. D. Johnson, D. C. Johnson, J. Am. Chem. Soc. 1996, 118, 2422–2426.
- [11] J. R. Williams, M. B. Johnson, D. C. Johnson, J. Am. Chem. Soc. 2001, 123 (8), 1645–1649.
- [12] J. R. Williams, M. B. Johnson, D. C. Johnson, J. Am. Chem. Soc. 2003, 125 (12), 3589-3592.
- [13] M. D. Hornbostel; E. J. Hyer; J. Thiel, D. C. Johnson, *Inorg. Chem.*, 1997, 36 (19), 4270–4274.
- [14] W. Heimbrodt, O. Goede, I. Tschentscher, V. Weinhold, A. Kli-makow, U. Pohl, K. Jacobs, N. Hoffmann, *Phys. B, Condens. Matter* 1993, 185, 357–361.
- [15] P. Tomasini, A. Haidoux, J. C. Tédenac, M. Maurin, J. Cryst. Growth 1998, 193, 572–576.
- [16] D. L. Decker, R. L. Wild, Phys. Rev. B 1971, 4, 3425–3437.
- [17] Q. Peng, Y. Dong, Z. Deng, H. Kou, S. Gao, Y. Li, J. Phys. Chem. B 2002, 106 (36), 9261–9265.
- [18] H. J. Chun, J. Y. Lee, D. S. Kim, S. W. Yoon, J. H. Kang, J. Park, J. Phys. Chem. C., 2007, 111 (2), 519–525.
- [19] L. Wang, L. Chen, T. Luo, K. Bao, Y. Qian, Solid State Commun. 2006, 138, 72–75.

- [20] M. Wu, Y. Xiong, N. Jiang, M. Ning, Q. Chen, J. Cryst. Growth 2004, 262, 567–571.
- [21] T. Qin, J. Lu, S. Wei, P. Qi, Y. Peng, Z. Yang, Y. Qian, *Inorg. Chem. Commun.* 2002, 5, 369–371.
- [22] D. J. Norris, N. Yao, F. T. Charnock, T. A. Kennedy, *Nano Letters* 2001, 1 (1), 3–7.
- [23] L. Levy, N. Feltin, D. Ingert, M. P. Pileni, J. Phys. Chem. B 1997, 101 (45), 9153–9160.
- [24] J. F. Suyver, S. F. Wuister, J. J. Kelly, A. Meijerink, *Nano Letters* 2001, 1 (8), 429–433.
- [25] J. M. Metha, P. G. Riewald, L. H. Vlack, J. Am. Ceram. Soc. 1967, 50, 164–164.
- [26] N. Elliott, J. Am. Chem. Soc. 1937, 59, 1958–1962.
- [27] H. Schnaase, Z. Phys. Chem. B 1933, 20, 89.
- [28] A. Baroni, Z. Kristallogr. 1938, 99, 336.
- [29] A. C. Zeppenfeld, S. L. Fiddler, W. K. Ham, B. J. Klopfenstein, C. J. Page, J. Am. Chem. Soc. 1994, 116, 9158–9165.
- [30] V. G. Vanyarkho, V. P. Zlomanov, A. V. Novoselova, V. N. Fokin, *Inorg. Mater.* 1969, 5, 1440–1443.
- [31] L. Fister, D. C. Johnson, J. Am. Chem. Soc. 1992, 114, 4639–4644.
- [32] D. M. Hamann, D. Bardgett, D. L. M. Cordova, L. A. Maynard, E. C. Hadland, A. C. Lygo, S. R. Wood, M. Esters, D. C. Johnson, Chem. Mater., 2018, 30 (18), 6209–6216.

Received: August 30, 2018

Published online: November 30, 2018